Vibration-assisted multiphoton resonance and multi-ion excitation

Wenjun Shao [1,2,3] Xun-Li Feng [4] Jian Li,[2,3] and Liang-Liang Wang [2,3,*]
[1]*Fudan University, Shanghai 200433, China*
[2]*Department of Physics, School of Science, Westlake University, Hangzhou 310024, China*
[3]*Institute of Natural Sciences, Westlake Institute for Advanced Study, Hangzhou 310024, China*
[4]*Department of Physics, Shanghai Normal University, Shanghai 200234, China*

(Received 13 July 2022; revised 2 November 2022; accepted 15 February 2023; published 4 April 2023)

We investigate the multiphoton resonance and multi-ion excitation in a single-mode cavity with identical vibrating ionqubits, which enables the tripartite interaction among the internal states of ions, the cavity mode and the ions' vibrational motion. Under particular resonant conditions, we derive effective Hamiltonians for the three-photon and the three-excitation cases, respectively, and find that the magnitude of the effective coupling energy can be tuned through the vibration mode, allowing for manipulations of ion-photon coupling in experiments. Furthermore, we analyze the system dynamics of our proposed setups and demonstrate the Rabi oscillation behaviors in these systems with dissipation effects. We propose our system as a versatile platform for the exploration of entangled multiqubit physics.

DOI: 10.1103/PhysRevResearch.5.023005

I. INTRODUCTION

The investigation of resonant emission of multiple photons [1–3] and resonant excitation of multiple atoms [4–6] is important not only due to the fundamental physics involved, but also because of their potential applications in, for example, the realization of quantum gates [7–11] and quantum information storage devices [12–14]. Following the first realization of two-photon absorption [15–18] in the 1960s and its rapid application [19–21] as a powerful spectroscopic and diagnostic tool, variant multiphoton processes have attracted growing research interests. Recently, Ma and Law [22] found that three photons can be simultaneously absorbed by a two-level atom in the strong coupling (SC) regime of Rydberg atoms confined in a high-Q cavity. On the other hand, Nori *et al.* [4,5] reported a counter-intuitive reverse phenomenon where a single photon can simultaneously excite two or more independent atoms in a symmetry-breaking potential.

Most existing investigations of multiphoton resonance and multiatom excitation processes assume the atoms to be static with the dipole approximation. With the development of atom and ion trapping techniques [23–25], however, the inclusion of the vibrational degrees of freedom of atoms in a cavity becomes increasingly important. The trapped ions [13,26,27] interacting with a quantized cavity field can be cooled down to their lowest vibrational state [28]. In such a cavity quantum electrodynamics (QED) system, the internal ionic states, the quantum vibration mode of the ion, and the single-mode cavity field are necessarily intertwined. For instance, Bužek *et al.* [28] analyzed the quantum motion of a cold, trapped two-level ion interacting with a quantized light field in a single-mode cavity. At zero temperature, the dynamics of a single trapped ion inside a nonideal QED cavity was studied by Rangel *et al.* [29]. Nevertheless, the effects of vibrational states in the multiphoton and multiatom processes remain unexplored to our knowledge.

In this work, we investigate a chain of trapped ions in a single-mode cavity and focus on the quantum effect of ionic vibration on the three-photon resonance and three-ion excitation processes in the cavity QED system. We derive effective Hamiltonians close to the resonance points and determine the energy level splittings. This reveals rich physics in our system. Although small vibrational frequency hardly affects the overall energy spectrum, the situation can be completely different and very interesting if the vibrating frequency is comparable to or larger than the ionic transition frequency. Remarkably, the energy splitting can be effectively controlled and enhanced by varying the vibration frequency, particularly around certain resonant conditions, resulting in vibrationally controlled ion-photon coherent manipulation. We further demonstrate the Rabi oscillation dynamics and discuss the associated damping effects, validating our analytical results with concrete numerical simulations.

This paper is organized as follows. In Sec. II, we describe the theoretical model of our scheme. Sections III and IV are devoted to study the vibration-assisted multiphoton resonance and multi-ion excitation, respectively, and Sec. V displays the quantum Rabi oscillations. In Sec. VI we give two examples of how to prepare N00N states and Greenberger-Horne-Zeilinger (GHZ) states. Finally, we end with discussion and conclusion in Sec. VII.

II. MODEL

We consider a chain of N identical ionqubits placed in a single-mode high-Q cavity [30,31]. As schematically shown

*wangliangliang@westlake.edu.cn

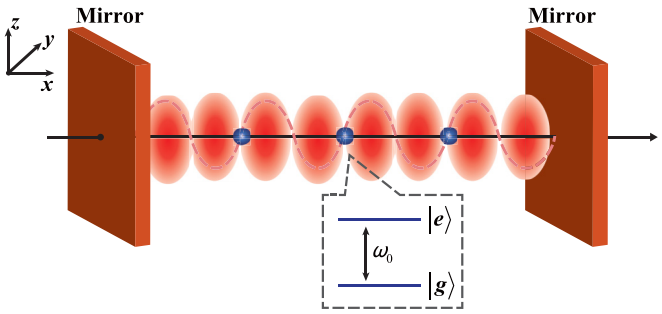

FIG. 1. Schematic diagram of a series of two-level ions trapped inside a standing-wave mode of an optical cavity. All ions are arranged at the nodes of the cavity's standing wave to make sure the tripartite coupling among the atomic internal states, the cavity mode and the vibrational motion to be the only relevant interaction.

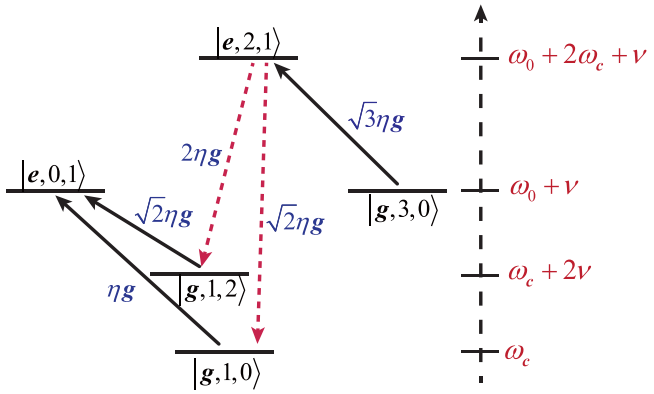

FIG. 2. Sketch of two paths contributing to the effective coupling between the bare states $|g, 3, 0\rangle$ and $|e, 0, 1\rangle$ via intermediate virtual transitions. The rotating processes are indicated by solid lines and the counter-rotating processes are indicated by dashed lines. The transition matrix elements are also displayed.

in Fig. 1, the trapped ions are assumed to sit close to the nodes of the cavity field standing wave, which can be best achieved by tuning the longitudinal trapping potential or the wavelength of the cavity field in the few-ion cases ($N \leqslant 3$). At the position of the node, the corresponding interaction Hamiltonian of the atomic internal states coupled to the cavity is $H_{\rm int} = \hbar g(\sigma_+ + \sigma_-)(b^\dagger + b)\sin(kx)$, where x is the displacement of ion from the node; k is the cavity wave vector; $b^\dagger$ (b) is the creation (annihilation) operator of the cavity field mode with the frequency ω_c; $\sigma_+ = |e\rangle\langle g|$ and $\sigma_- = |g\rangle\langle e|$ are Pauli matrices for the two-level ion; g represents the coupling strength between the cavity mode and the ionic internal states $|e\rangle$ and $|g\rangle$ [32]. Any ion-light coupling cannot be evoked without the motional excursion of the ion away from the node. Consequently, the tripartite coupling among the atomic internal states, the cavity mode, and the vibrational motion of the ions, become the only allowed interaction [32–34]. We will consider the lowest collective mechanical mode of the ions [7,8,35], which is referred to as the center-of-mass mode. The fully quantized Hamiltonian of the system thus reads (we set $\hbar = 1$) [31–34]

$$H = H_0 + H_{\rm int}, \tag{1}$$

$$H_0 = \nu a^\dagger a + \omega_c b^\dagger b + \tfrac{1}{2}\omega_0 J_z, \tag{2}$$

$$H_{\rm int} = g\sin[\eta(a^\dagger + a)](J_+ + J_-)(b^\dagger + b), \tag{3}$$

where $a^\dagger$ (a) is the creation (annihilation) operator of the ion center-of-mass mode with frequency ν; $J_\pm = \sum_i \sigma_\pm^i$ and $J_z = \sum_i \sigma_z^i = \sum_i(|e_i\rangle\langle e_i| - |g_i\rangle\langle g_i|)$ operate on the ionic twolevels with transition frequency ω_0; $\eta = k\Delta x$ is the Lamb-Dicke parameter, Δx being the amplitude of the harmonic motion with $x = \Delta x(a^\dagger + a)$ [29]. In the case of strong confinement, the Lamb-Dicke condition $\eta \ll 1$ is naturally satisfied and the interaction Hamiltonian can be transformed conveniently to a trilinear form $H_{\rm int} \approx g\eta(a^\dagger + a)(J_+ + J_-)(b^\dagger + b)$ with the approximation $\sin[\eta(a^\dagger + a)] \approx \eta(a^\dagger + a)$. Note that the high-order resonant transitions that are of our particular interest in this paper can be realized via intermediate states connected by counter-rotating terms (CRTs) in the interaction Hamiltonian, such as $a\sigma_+ b^\dagger$, which describes the creation of a photon in the cavity accompanied by an ionic excitation from its ground state together with the annihilation of a phonon from the ionic vibration.

III. ENERGY SPLITTING CONTROLLED BY VIBRATIONAL MODE

For the sake of simplicity, we first investigate the single ion case with $N = 1$. Under the resonant condition with $\omega_c \approx (\omega_0 + \nu)/3$, the dominant coupling terms are $a^\dagger b^3\sigma_+$ and $a(b^\dagger)^3\sigma_-$, describing the ion excited from its ground state by annihilating three photons while creating one phonon, as well as its inverse process. As illustrated in Fig. 2, the presence of CRTs in the interaction Hamiltonian enables two different paths for the transitions $|g, 3, 0\rangle \leftrightarrow |e, 0, 1\rangle$. Here and in what follows, kets list qubit state, photon excitation number, followed by phonon excitation number. By applying standard third-order perturbation theory [6,36], we obtain the effective coupling strength between bare states $|g, 3, 0\rangle$ and $|e, 0, 1\rangle$, under the resonant condition $3\omega_c = \omega_0 + \nu$, to be

$$\Omega_{\rm eff} = \frac{27\sqrt{6}(\eta g)^3\omega_0}{4(\omega_0 + \nu)^2(\omega_0 - 2\nu)}. \tag{4}$$

The effective interaction Hamiltonian of interest is $H_{\rm eff} = -\Omega_{\rm eff}(|e, 0, 1\rangle\langle g, 3, 0| + \text{H.c.})$. Typically, $2\Omega_{\rm eff}$ can be understood as the energy splitting at the avoided crossing (see Fig. 3), which originates from the hybridization of the states $|g, 3, 0\rangle$ and $|e, 0, 1\rangle$.

Clearly, when ν is small compared with the ionic transition frequency ω_0, $2\Omega_{\rm eff}/\omega_0$ is proportional to the cubic of the coupling coefficient, i.e., $2\Omega_{\rm eff}/\omega_0 \sim (\eta g)^3/\omega_0^3$. Therefore, in order to observe this energy splitting, the ultra-strong coupling (USC) [37,38] or even deep-strong coupling (DSC) regime [39], is required to ensure that the effective coupling induced by the higher-order processes becomes larger than the relevant decoherence rate in the system. In Fig. 3, we further compare analytically obtained Eq. (4) with the energy splitting $2\Omega_{\rm eff}/\omega_0$ obtained from numerically diagonalizing the original Hamiltonian at different $\eta g/\omega_0$. The results from

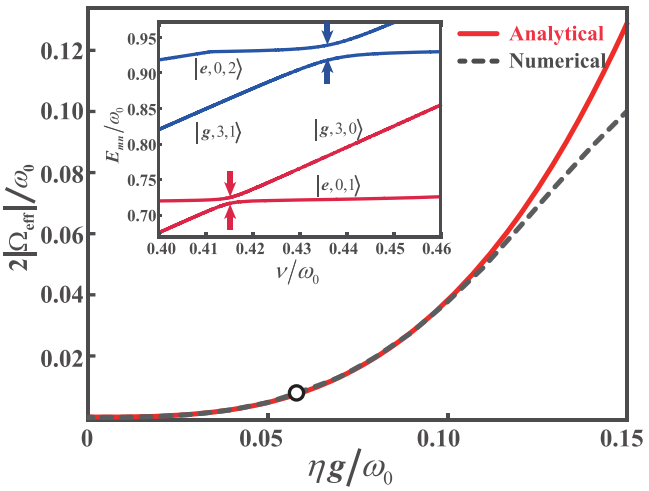

FIG. 3. Comparison of the effective energy splitting $2|\Omega_{\rm eff}|/\omega_0$ obtained analytically (solid red line) and numerically (dashed line) as a function of interaction strength $\eta g/\omega_0$ with $\nu/\omega_0 = 0.2$. The inset shows the energy spectrum for states: $|g, 3, 0\rangle \leftrightarrow |e, 0, 1\rangle$ and $|g, 3, 1\rangle \leftrightarrow |e, 0, 2\rangle$ at $\eta g/\omega_0 = 0.06$ marked by the black circle. The avoided-level crossings indicated by the arrows occur with the energy splitting about $0.008\omega_0$ and $0.021\omega_0$, respectively. The corresponding positions of resonance are $0.415\omega_0$ and $0.437\omega_0$.

the two methods agree very well at relatively small coupling (the percentage difference is lower than 2% for $\eta g/\omega_0 < 0.1$), validating our perturbation theory formula Eq. (4) as a good approximation. We note that the above results can be generalized to other pairs of bare states $|g, m, n\rangle$ and $|e, m-3, n+1\rangle$, where m (n) denotes the photon (phonon) number, and the energy splitting can be formally enhanced with a larger number of photons or phonons [40].

When the vibrational frequency is comparable to or larger than the ionic transition frequency and the cavity mode frequency, the picture can be complicated by the additional longitudinal modes of the cavity generated due to the rapid ionic vibration [34]. In this regard, the capability of the cavity to maintain a single mode [31] is particularly useful for us to neglect such a complication in our following discussion. To achieve a more prominent energy splitting, we consider the vibrational frequency in the regime $0 < \nu < \omega_0$. As shown in Fig. 4(a), the perturbative result in Eq. (4) suggests a divergence of the effective coupling $\Omega_{\rm eff}$ at $\nu/\omega_0 = 1/2$, which is regularized in the numerical calculation as a pronounced but finite peak. This divergence point is indeed where the perturbation theory breaks down because of the occurrence of higher level degeneracy involving other states than the two original states in our problem. Specifically, for the case with the initial state $|g, 3, 0\rangle$ or $|e, 0, 1\rangle$, the presumed intermediate state $|g, 1, 2\rangle$ becomes energetically aligned with these two states in the decoupled limit when $\nu/\omega_0 = 1/2$, such that the coupling will lead to hybridization of all three states (see Appendix A) and both our perturbation theory and the two-level resonance picture will fail close to this point. Hence we introduce a fidelity measure for the two-state transition, which is defined by the total probability weights of the two relevant states $|g, 3, 0\rangle$ and $|e, 0, 1\rangle$. In Fig. 4(b), we show the line contours for where this fidelity is equal to 90%

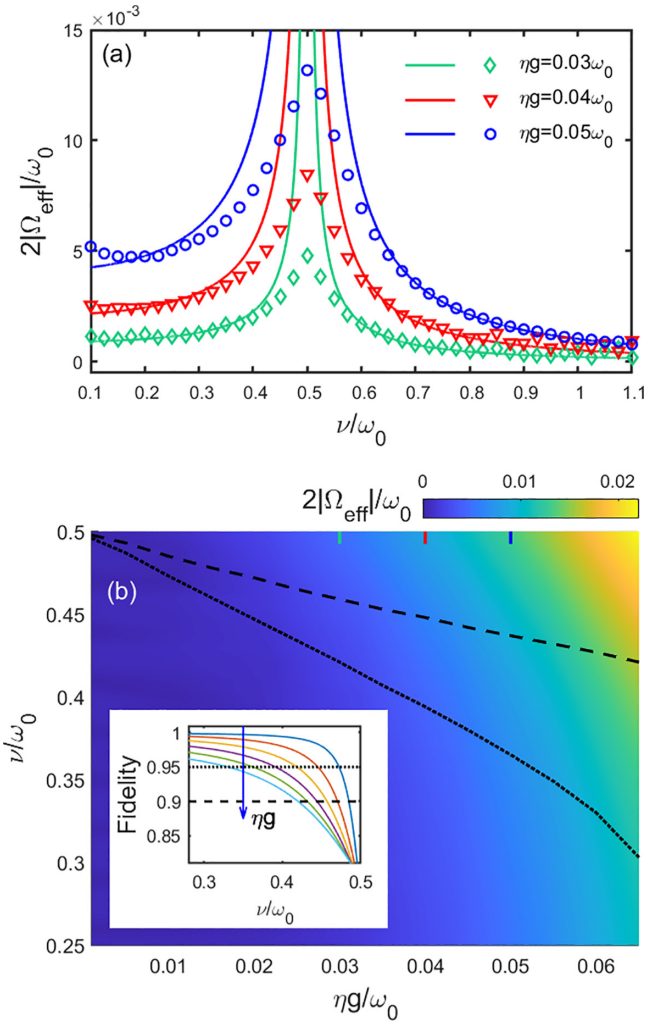

FIG. 4. (a) Energy splitting $2|\Omega_{\rm eff}|/\omega_0$ of $|g, 3, 0\rangle \leftrightarrow |e, 0, 1\rangle$ obtained numerically as a function of ν/ω_0 for $\eta g = 0.03\omega_0$ (green diamond), $\eta g = 0.04\omega_0$ (red triangle), and $\eta g = 0.05\omega_0$ (blue circle), as well as the corresponding analytical results (solid lines). Note that the numerical results show finite peaks at the analytically divergent point at $\nu/\omega_0 = 0.5$. (b) The numerically-calculated resonant energy splitting in the $\nu - \eta g$ plane. The inset shows the fidelity, defined as the average probability weights on the states $|g, 3, 0\rangle$ and $|e, 0, 1\rangle$, under the resonant condition for ηg varying from $0.01\omega_0$ to $0.06\omega_0$ (lines from top to bottom). The 90% and 95% fidelity levels are indicated in both the main plot and the inset by the dashed and the dotted lines, respectively. In the main plot, the three values of ηg considered in panel (a) are also marked with short line segments of corresponding colors.

(the dashed line) and 95% (the dotted line), respectively. By following such contours, optimized values of the interaction strength ηg and the vibrational frequency ν can be found with a specific fidelity threshold. It is quite interesting that the energy splitting can be greatly enhanced by the ionic vibration mode, making high-order resonant transitions significant for realistic experimental parameters. As we will see below, such enhanced energy splitting also appears in the system with multiple trapped ions.

IV. VIBRATION-ASSISTED MULTI-ION EXCITATION PROCESS

We now turn to study a chain of $N = 3$ ions and discuss a specific multi-ion excitation process: one photon and one phonon can be jointly absorbed by three ions. Following similar procedures as in the above section and utilizing the generalized James' effective Hamiltonian method [41], we arrive at

$$H_{\text{eff}} = -\Omega_{\text{eff}}[ab\sigma_+^1\sigma_+^2\sigma_+^3 + a^\dagger b^\dagger \sigma_-^1\sigma_-^2\sigma_-^3], \tag{5}$$

with

$$\frac{\Omega_{\text{eff}}}{\omega_0} = \frac{3\nu(3\omega_0 - \nu)}{2(\omega_0 - \nu)(2\omega_0 - \nu)}\left(\frac{\eta g}{\omega_0}\right)^3 \tag{6}$$

being the effective coupling strength for the transition between the states $|ggg, 1, 1\rangle$ and $|eee, 0, 0\rangle$, where the simultaneous excitation condition $\omega_c = 3\omega_0 - \nu$ has been taken. The above result resembles that in the case of simultaneous excitation of three ions by only one photon, except that in the latter case the strength of the effective coupling between $|ggg, 1\rangle$ and $|eee, 0\rangle$ vanishes on resonance $\omega_c = 3\omega_0$ (discussed in Ref. [4] and the case IV B2(c) of Ref. [6]) because of the destructive interfere between different transition paths. By contrast, the energy splitting will be finite on resonance as long as the transition is assisted by a vibration mode (see Appendix B). In addition, similar to the preceding three-photon resonance process, the energy splitting implied by Eq. (6) shows two divergences at $\nu/\omega_0 = 1, 2$, which indicate the breaking down of the perturbation theory and are regulated in the numerical results as two pronounced peaks.

V. SYSTEM DYNAMICS

In order to better demonstrate the processes we have proposed, we now describe the system dynamics with all the dissipation channels taken into account. Here, we adopt the master equation approach following Refs. [3–5,42–46] as the standard quantum optical master equation breaks down in the USC regime. With the Born-Markov approximation and assuming the system interacting with zero-temperature baths, the Lindblad master equation (see Appendix C) regarding our system is given by

$$\begin{aligned}\dot{\rho}(t) = & -i[H, \rho(t)] + \kappa\mathcal{D}[X^+]\rho(t) \\ & + \gamma\sum_i \mathcal{D}[C_i^+]\rho(t) + \zeta\mathcal{D}[P^+]\rho(t),\end{aligned} \tag{7}$$

where the Lindblad superoperator $\mathcal{D}$ is defined as $\mathcal{D}[O]\rho = \frac{1}{2}(2O\rho O^\dagger - \rho O^\dagger O - O^\dagger O\rho)$ with $O = \sum_{j,k>j}\langle j|(o + o^\dagger)|k\rangle|j\rangle\langle k|$ in terms of the energy eigenstates $|j\rangle$ of the system Hamiltonian H being the dressed lowering operator (positive frequency part) for the cavity field ($o = b$, $O = X^+$), the vibration mode ($o = a$, $O = P^+$), and the ith ion ($o = \sigma_-^i$, $O = C_i^+$), respectively. We choose the labeling of the states $|j\rangle$ (to avoid unphysical effects) such that $\omega_k > \omega_j$ for $k > j$ [5,43]. Correspondingly, for the negative frequency part, $O^\dagger = X^-$, P^- or C_i^-. The constants κ, ζ, and γ correspond to the damping rates for the cavity mode, the vibration mode, and the ions, respectively.

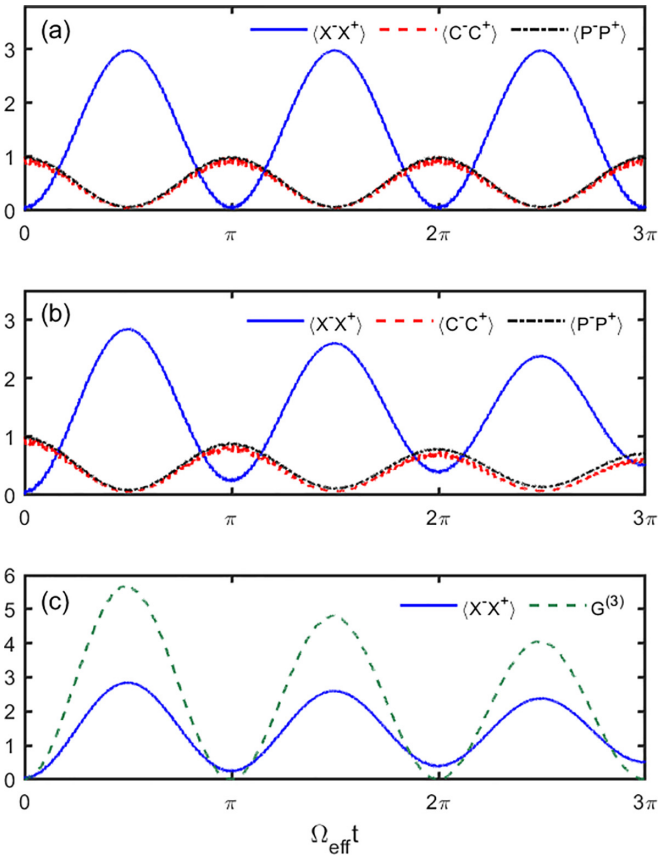

FIG. 5. Time evolution of the ion mean excitation number $\langle C^-C^+\rangle$ (red dashed curve), the cavity mean photon number $\langle X^-X^+\rangle$ (blue solid curve), the three-photon correlation function $G^{(3)}$ (green dashed curve), and the mean phonon number $\langle P^-P^+\rangle$ (black dot dashed curve) with (a) no decay and (b), (c) decay rates $\kappa = \gamma = 2\zeta = 1\times10^{-4}\omega_0$, respectively. The initial state is taken to be $|e, 0, 1\rangle$ and the other parameters are $\eta g/\omega_0 = 0.06$ and $\nu/\omega_0 = 0.15$.

For the case of three-photon resonance, the system is initially prepared in the state $|e, 0, 1\rangle$. Figure 5 shows the time evolution of the ion mean excitation number $\langle C^-C^+\rangle$, the cavity mean photon number $\langle X^-X^+\rangle$, the three-photon correlation function $G^{(3)} = \langle X^-X^-X^-X^+X^+X^+\rangle$, and the mean phonon number $\langle P^-P^+\rangle$. In the ideal case without dissipation [Fig. 5(a)], the mean photon number at its maximum approaches three; meanwhile, the ion transits to its ground state and the mean phonon number approaches zero, which is a signature of the cavity mode being in a three-photon state excited by the ion and one phonon. This process is reversible accompanied by energy exchanges. When the dissipation effect is included in the system dynamics [Fig. 5(b)], the mean values oscillate with the time evolution but decrease exponentially in their amplitudes as expected. To get an essentially deterministic transfer, Ω_{eff} should far exceed the relevant damping rates κ, ζ and γ. In Fig. 5(c) we observe that the peak values of $G^{(3)}$ are approximately twice of the mean photon number $\langle X^-X^+\rangle$ in the first transition cycle, indicating an almost-perfect three-photon correlation [3]. Similarly, the Rabi oscillation of multi-ion excitation (see Appendix D) also shows a reversible energy exchange with the decay rate of

its amplitudes depending on the relative strength between the effective coupling and the system loss.

VI. CONSTRUCTION OF N00N STATES AND GHZ STATES

By tuning the cavity frequency, we can construct an assortment of entangled states [9], such as N00N states and GHZ states. Firstly, we construct the N00N states in the investigation of a simple multiphoton case: three photons excite one ion accompanied with the creation of three phonons. By applying the third-order perturbation theory with $\omega_c = (\omega_0 + 3\nu)/3$, we find there only exists a path connecting the specific states $|g, 3, 0\rangle$ and $|e, 0, 3\rangle$, and the effective coupling strength is $\Omega_{\text{eff}} = 27(\eta g)^3/2\omega_0^2$. To construct a N00N entangled state, one may prepare the trapped ion in a coherent superposition of two energy eigenstates $|\varphi\rangle = \cos\theta|e\rangle + e^{i\phi}\sin\theta|g\rangle$. Meanwhile, the cavity state is prepared to vacuum state, and the ionic motional state is in three-phonon state. So we have the following state vector for the ion-field state

$$|\Psi\rangle(0) = (\cos\theta|e\rangle + e^{i\phi}\sin\theta|g\rangle)|0, 3\rangle. \tag{8}$$

At a time t, the ion-field state vector will become

$$|\Psi\rangle(t) = \cos\theta[\cos(\Omega_{\text{eff}}t)|e, 0, 3\rangle - i\sin(\Omega_{\text{eff}}t)|g, 3, 0\rangle] + e^{i\phi}\sin\theta|g, 0, 3\rangle. \tag{9}$$

Once interaction time t satisfies $t_k = \pi(4k + 3)/2\Omega_{\text{eff}}$ ($k = 0, 1, 2, \ldots$), the resulting state is

$$|\Psi(t_k)\rangle = i\cos\theta|g, 3, 0\rangle + e^{i\phi}\sin\theta|g, 0, 3\rangle. \tag{10}$$

If measuring the ion in its internal state $|g\rangle$ for equally weighted ionic states ($\theta = \pi/4$), we finally get a N00N state with $N = 3$:

$$|\psi\rangle = \frac{1}{\sqrt{2}}(i|3, 0\rangle + e^{i\phi}|0, 3\rangle), \tag{11}$$

where the phase ϕ is fully transferred from the ionic superposition states $|\varphi\rangle$ [33]. As a source of entanglement, the N00N states are often used for performing high-precision measurements.

In the multi-ion excitation process, a multiqubit type GHZ state can be constructed, which is highly sought for applications to quantum communication and information. Under the resonant condition $\omega_c = 3\omega_0 + \nu$, the dominant coupling give a description of simultaneous excitation of three ions and one phonon triggered by one photon. $\Omega_{\text{eff}} = \frac{3\nu(3\omega_0+\nu)(\eta g)^3}{2\omega_0^2(\omega_0+\nu)(2\omega_0+\nu)}$ is the effective coupling strength for the transition between the bare states $|ggg, 1, 0\rangle$ and $|eee, 0, 1\rangle$. Consider that the cavity state is prepared in a coherent superposition state $|\varphi\rangle = \cos\theta|1\rangle + e^{i\phi}\sin\theta|0\rangle$ and both three trapped ions and ionic motional state are prepared to ground states; the initial state of the system is given by

$$|\Psi\rangle(0) = |ggg\rangle(\cos\theta|0\rangle + e^{i\phi}\sin\theta|1\rangle)|0\rangle, \tag{12}$$

then we have

$$|\Psi\rangle(t) = \cos\theta[\cos(\Omega_{\text{eff}}t)|ggg, 1, 0\rangle - i\sin(\Omega_{\text{eff}}t)|eee, 0, 1\rangle] + e^{i\phi}\sin\theta|ggg, 0, 0\rangle. \tag{13}$$

Clearly, if one measures the cavity photon in its vacuum state when $t_k = \pi(4k + 3)/2\Omega_{\text{eff}}$ ($k = 0, 1, 2, \ldots$) with $\theta = \pi/4$, the resulting state will become a GHZ_4 state:

$$|\psi\rangle = \frac{1}{\sqrt{2}}(e^{i\phi}|ggg, 0\rangle + i|eee, 1\rangle). \tag{14}$$

It is different to the case shown in Ref. [4], in which only a hybrid entangled GHZ state, i.e., $(|gg, 1\rangle + |ee, 0\rangle)/\sqrt{2}$, can be obtained without atomic vibration. In our system including the quantum vibrational mode, a tetrapartite and fully correlated GHZ state [Eq. (14)] can be constructed in a remarkably simple way.

VII. DISCUSSION AND CONCLUSION

For the case we have discussed with $N = 1, 3$, the ions are assumed to be distributed uniformly [47–49] in a Radio-Frequency (RF) linear Paul trap [50]. The ions are strongly bound in radial directions and weakly bound in a harmonic potential in the axial direction. The equilibrium position of the ion is determined by the joint effect of the overall harmonic trap and the Coulomb force, and the ion-ion distance can be tuned via the trap frequency. To achieve the vibration frequency [51,52] of the ion comparable to the cavity field frequency and ionic transition frequency, a microwave cavity with resonant frequency in the MHz spectral range is adopted and a suited Rydberg transition of Rb ions can be achieved [53], which is feasible with current existing techniques. Moreover, in the USC or DSC regimes the coupling constant $g/\omega_0 = 0.1 \sim 1$, thus the effective coupling strength Ω_{eff} can be the order of kHz and even larger. As quantum circuit has advantages of tunability and flexibility, our model can be simulated in the circuit QED experiments [54,55], in which the relevant decay rates $\kappa = \gamma = 2\zeta = 10^{-4}\omega_0$ are available [56,57]. In perspective, with the development and improvement of the experimental setup applied in cavity QED experiments [52,58], our proposal would be realized with a large probability in the nearest future. A noteworthy issue is that with increasing number of ions ($N > 3$), the ion distribution in a RF trap becomes inhomogeneous and the ion-ion distance increases from the trap center to the edges. For a system involving only a small number of ions such as in our proposals, however, we expect the ion-ion distance only varies insignificantly and the equilibrium positions of the ions are still close enough to the nodes of the cavity standing wave. Recently, a technique [49,59] has been developed to realize an uniform ion distribution in a long range by controlling the electrode voltage of a surface ion trap, which may also be adapted for implementations of our proposals.

We have investigated the cavity QED with vibrating two-level ions in the large-detuning regime, focusing on two phonon-assisted phenomena: three-photon resonance and three-ion simultaneous excitation. Such cavity QED systems can be used to prepare complex entangled states such as the N00N states and the GHZ states, or to realize threebody effective interaction [60–62] among trapped ions. With the state-of-the-art techniques in optical lattices, circuit QED systems [54,55], and optomechanical systems [63,64], we expect our proposals can be generalized (see Appendix E) to various experimental platforms with coupling between qubits and

multiple types of bosons such as resonator modes, optical or acoustic phonons [65], thus providing more insights into quantum entanglement physics and promoting the further development of novel quantum technology.

ACKNOWLEDGMENTS

We would like to thank Chunfeng Wu, Yong Sun, Chang-An Li, and Jinxing Hou for interesting discussions. This work was supported by foundation of Zhejiang Province Natural Science under Grant No. LQ20A040002. J.L. acknowledges support from National Natural Science Foundation of China under Project 11774317.

APPENDIX A: EFFECTIVE THREE-LEVEL HAMILTONIAN

By adjusting the frequency $\nu \sim \omega_0/2$, three energy levels $|e,0,1\rangle$, $|g,3,0\rangle$, and $|g,1,2\rangle$ become degenerate instead of two. We can expect something different. In this Appendix, we present the full adiabatic elimination calculations [3,22,46] for the degenerate three levels and give rise to an effective three level Hamiltonian describing the hybridization between those degenerate levels. Starting from the truncated levels shown in Fig. 2, we move to a frame rotating with $\omega_0+\nu$, i.e., subtracting $\omega_0+\nu$ from the diagonal of the Hamiltonian, giving

$$H=\begin{pmatrix} 2\omega_c & 0 & \sqrt{3}\eta g & 2\eta g & \sqrt{2}\eta g \\ 0 & 0 & 0 & \sqrt{2}\eta g & \eta g \\ \sqrt{3}\eta g & 0 & 3\omega_c-\omega_0-\nu & 0 & 0 \\ 2\eta g & \sqrt{2}\eta g & 0 & \omega_c-\omega_0+\nu & 0 \\ \sqrt{2}\eta g & \eta g & 0 & 0 & \omega_c-\omega_0-\nu \end{pmatrix}, \tag{A1}$$

where the states are ordered as $|e,2,1\rangle$, $|e,0,1\rangle$, $|g,3,0\rangle$, $|g,1,2\rangle$, and $|g,1,0\rangle$. Denoting the amplitudes of the five states by c_1-c_5, respectively, the Schrödinger equation gives

$$i\dot{c}_j=\sum_{i,j=1}^{5} H_{ji}c_i. \tag{A2}$$

Assuming that $3\omega_c \sim \omega_0+\nu$, $\nu\sim\omega_0/2$ and $\eta g \ll 2\omega_c, \omega_c-\omega_0-\nu$, we can adiabatically eliminate the two intermediate levels and their population will not change significantly, i.e., $\dot{c}_1=\dot{c}_5=0$, thus we give

$$c_1=-\frac{9\sqrt{2}(\eta g)^2}{18(\eta g)^2+4(\omega_0+\nu)^2}c_2-\frac{3\sqrt{3}\eta g(\nu+\omega_0)}{9(\eta g)^2+2(\omega_0+\nu)^2}c_3-\frac{6\eta g(\nu+\omega_0)}{9(\eta g)^2+2(\omega_0+\nu)^2}c_4, \tag{A3}$$

$$c_5=\frac{3\eta g(\omega_0+\nu)}{9(\eta g)^2+2(\omega_0+\nu)^2}c_2-\frac{9\sqrt{6}(\eta g)^2}{18(\eta g)^2+4(\omega_0+\nu)^2}c_3-\frac{9\sqrt{2}(\eta g)^2}{9(\eta g)^2+2(\omega_0+\nu)^2}c_4. \tag{A4}$$

Then we insert into the equations for c_2, c_3, and c_4 and the effective three-level Hamiltonian is shown to be

$$H_{\text{eff}}=\begin{pmatrix} \frac{3(\eta g)^2(\omega_0+\nu)}{9(\eta g)^2+2(\omega_0+\nu)^2} & -\frac{9\sqrt{6}(\eta g)^3}{18(\eta g)^2+4(\omega_0+\nu)^2} & \frac{2\sqrt{2}\eta g(\nu+\omega_0)^2}{9(\eta g)^2+2(\omega_0+\nu)^2} \\ -\frac{9\sqrt{6}(\eta g)^3}{18(\eta g)^2+4(\omega_0+\nu)^2} & -\frac{9(\eta g)^2(\nu+\omega_0)}{9(\eta g)^2+2(\omega_0+\nu)^2} & -\frac{6\sqrt{3}(\eta g)^2(\nu+\omega_0)}{9(\eta g)^2+2(\omega_0+\nu)^2} \\ \frac{2\sqrt{2}\eta g(\nu+\omega_0)^2}{9(\eta g)^2+2(\omega_0+\nu)^2} & -\frac{6\sqrt{3}(\eta g)^2(\omega_0+\nu)}{9(\eta g)^2+2(\omega_0+\nu)^2} & \frac{2}{3}\omega_0+\frac{4}{3}\nu-\frac{12(\eta g)^2(\nu+\omega_0)}{9(\eta g)^2+2(\omega_0+\nu)^2} \end{pmatrix}. \tag{A5}$$

If the frequency ν is far away from the half of the transition ω_0, by applying standard perturbation theory again, we can obtain more exact effective coupling strength between bare states $|g,3,0\rangle$ and $|e,0,1\rangle$ to be

$$\Omega_{\text{eff}}=\frac{27\sqrt{6}(\eta g)^3\omega_0}{54(\eta g)^2\omega_0-4(\omega_0+\nu)^2(\omega_0-2\nu)}. \tag{A6}$$

Clearly, when ν is close to the divergence point $\nu/\omega_0=1/2$ of the former effective coupling Ω_{eff} [Eq. (4)], there is a pronounced and finite peak $\sim\sqrt{6}\eta g/2$. This expression is a much better approximation to the exact value, which provides a more accurate analytical description of Fig. 4.

APPENDIX B: COMPARISON OF THE EFFECTIVE COUPLING STRENGTHS WITH AND WITHOUT VIBRATION

According to the standard perturbation theory [4,6,36], the magnitude of the effective coupling between two bare states $|i\rangle$ and $|f\rangle$ is expressed as

$$\Omega_{\text{eff}}=\sum_{j_1,j_2\cdots j_{n-1}}\frac{V_{fj_{n-1}}\cdots V_{j_2j_1}V_{j_1i}}{(E_i-E_{j_1})(E_i-E_{j_2})\cdots(E_i-E_{j_{n-1}})}, \tag{B1}$$

where E_{j_n} represents the energy of the bare state $|j_n\rangle$, while $V_{j_nj_{n+1}}=\langle j_n|H_{\text{int}}|j_{n+1}\rangle$. The sum goes over all of the virtual transition steps which forms a transition path connecting the initial state $|i\rangle$ to the final state $|f\rangle$. As presented in Ref. [6],

the effective coupling strength between the states $|eee, 0\rangle$ and $|ggg, 1\rangle$, representing the simultaneous excitation of three atoms with a single photon, is

$$\Omega_{\text{eff}} = -\frac{3g^3(\omega_c - 3\omega_0)}{\omega_0(\omega_c - \omega_0)^2}. \tag{B2}$$

Apparently, such a coupling between the states $|eee, 0\rangle$ and $|ggg, 1\rangle$ nevertheless exists close to the resonance ($\omega_c = 3\omega_0$), which has been substantiated by the numerical calculations when the two states are slightly out of resonance in the Supplemental Material of Ref. [4].

By contrast, the effective coupling strength will never go to zero on resonance in our system due to the involvement of a vibration mode in the process of simultaneously exciting three ions with one photon. Specifically, we consider a case in which three ions are simultaneously excited by a photon and a phonon. The effective coupling strength between $|eee, 0, 0\rangle$ and $|ggg, 1, 1\rangle$ has a complex form

$$\Omega_{\text{eff}} = \frac{3(\eta g)^3}{\omega_0}\left(\frac{1}{\omega_0 - \omega_c - \nu} + \frac{2}{\omega_0 - \omega_c + \nu} + \frac{2}{\omega_0 + \omega_c - \nu} + \frac{4}{\omega_0 + \omega_c + \nu}\right), \tag{B3}$$

which gives a nonzero outcome under the resonance condition $\omega_c = 3\omega_0 - \nu$, just being equivalent to the Ω_{eff} in Eq. (6). A similar result can be obtained in the case that one photon can simultaneously excite three ions and one phonon. The effective coupling strength for the transition between the states $|eee, 0, 1\rangle$ and $|ggg, 1, 0\rangle$ is

$$\Omega_{\text{eff}} = 3(\eta g)^3\left(\frac{1}{\omega_0 - \omega_c + \nu} + \frac{2}{\omega_0 + \omega_c + \nu}\right)\left(\frac{1}{\omega_0} + \frac{2}{\omega_0 + \nu}\right), \tag{B4}$$

which also never go to zero on resonance ($\omega_c = 3\omega_0 + \nu$).

APPENDIX C: MASTER EQUATION

Here, we briefly present some key points to derive the master equation. First, we consider a generic system, which consists of N interacting subsystems or components. Each nth subsystem is assumed to be coupled to an independent bath of quantum harmonic oscillators, with the free Hamiltonian [43]

$$H_B^{(n)} = \sum_l \omega_l c_{n,l}^\dagger c_{n,l}, \tag{C1}$$

where $c_{n,l}^\dagger$ and $c_{n,l}$ are bosonic creation and annihilation operators for the $l$bath mode with frequency ω_l of the nth reservoir. The interaction between the system and the oscillator baths is describes by

$$H_{SB} = \sum_{n,l} \alpha_{n,l}(s_n + s_n^\dagger)(c_{n,l} + c_{n,l}^\dagger), \tag{C2}$$

where $s_n^\dagger$ (s_n) are creation (annihilation) operators of the nth subsystem. For the ion-qubit $s_n \to \sigma_-$, while for the bosonic mode (photon or phonon) $s_n \to a, b$. $\alpha_{n,l}$ denotes the coupling strength between the nth subsystem and the bath mode l of the nth reservoir. In the interaction picture, the system-bath interaction Hamiltonian is given by

$$\tilde{H}_{SB} = \sum_{n,l} \alpha_{n,l} e^{iH_S t}(s_n + s_n^\dagger)e^{-iH_S t}(c_{n,l}e^{-i\omega_l t} + c_{n,l}^\dagger e^{i\omega_l t}), \tag{C3}$$

in which H_S is the system Hamiltonian. Expressing H_S in the dressed basis of its energy eigenstates $|j\rangle$, then we write the system operators in the interaction picture as

$$\tilde{S}_n(t) = \sum_{j,k>j} C_{jk}|j\rangle\langle k|e^{i\Delta_{jk}t}, \tag{C4}$$

with

$$C_{jk} = \langle j|(s_n + s_n^\dagger)|k\rangle, \tag{C5}$$

$$\Delta_{jk} = E_j - E_k, \tag{C6}$$

and the reservoir operators as

$$\tilde{B}_n(t) = \sum_{n,l} \alpha_{n,l} c_{n,l} e^{-i\omega_l t}. \tag{C7}$$

Here the " ~ " sign identifies the operators in the interaction picture. As shown in detail in Ref. [42], $C_{jj} = 0$, as the considered system in this case has parity symmetry. Then dropping the fast oscillating terms $\tilde{S}_n^\dagger(t)\tilde{B}_n^\dagger(t)$ and $\tilde{S}_n(t)\tilde{B}_n(t)$ by the rotating-wave approximation, we find Eq. (C3) can be simplified as

$$\tilde{H}_{SB} = \sum_n [\tilde{S}_n(t)\tilde{B}_n^\dagger(t) + \tilde{S}_n^\dagger(t)\tilde{B}_n(t)]. \tag{C8}$$

By Born-Markov approximation, the dressed master equation for the system becomes [22,42]

$$\begin{aligned}\dot{\tilde{\rho}}_s(t) = \sum_{m,n}\Bigg\{&\int_0^t dt'[\tilde{S}_n(t')\tilde{\rho}_s(t')\tilde{S}_m(t) - \tilde{S}_m(t)\tilde{S}_n(t')\tilde{\rho}_s(t')]\langle\tilde{B}_m^\dagger(t)\tilde{B}_n^\dagger(t')\rangle + \int_0^t dt'[\tilde{S}_n(t')\tilde{\rho}_s(t')\tilde{S}_m^\dagger(t)\\ &- \tilde{S}_m^\dagger(t)\tilde{S}_n(t')\tilde{\rho}_s(t')]\langle\tilde{B}_m(t)\tilde{B}_n^\dagger(t')\rangle + \int_0^t dt'[\tilde{S}_n^\dagger(t')\tilde{\rho}_s(t')\tilde{S}_m(t) - \tilde{S}_m(t)\tilde{S}_n^\dagger(t')\tilde{\rho}_s(t')]\langle\tilde{B}_m^\dagger(t)\tilde{B}_n(t')\rangle\\ &+ \int_0^t dt'[\tilde{S}_n^\dagger(t')\tilde{\rho}_s(t')\tilde{S}_m^\dagger(t) - \tilde{S}_m^\dagger(t)\tilde{S}_n^\dagger(t')\tilde{\rho}_s(t')]\langle\tilde{B}_m(t)\tilde{B}_n(t')\rangle\Bigg\} + \text{H.c.}.\end{aligned} \tag{C9}$$

Each term of which embodies oscillating exponentials of the form $\exp[i(\Delta_{jk} - \Delta_{j'k'})t]$. For pairs of different transitions occurring at the same frequency, or for $j = j'$ and $k = k'$ (since $k > j$ and $k' > j'$), the argument of these

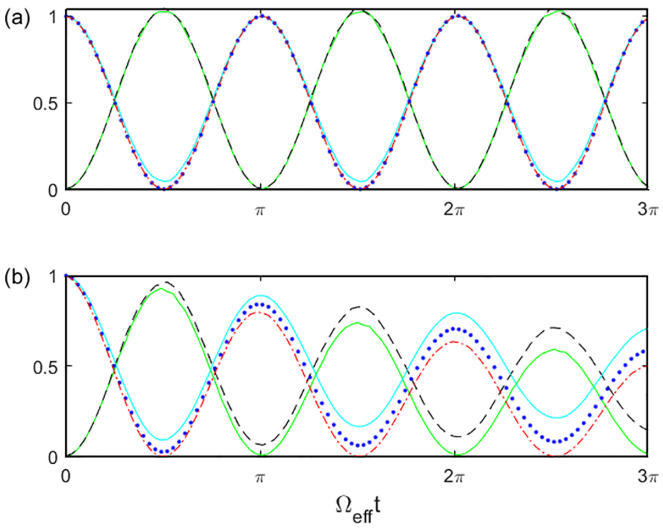

FIG. 6. Time evolution of the cavity mean photon number $\langle X^- X^+ \rangle$ (green solid curve), the ion 1 mean excitation number $\langle C_1^- C_1^+ \rangle$ (cyan dashed curve), the zero-delay two-ion correlation function $S^{(2)}$ (blue dotted curve), the zero-delay three-ion correlation function $S^{(3)}$ (red dot-dashed curve) and the mean phonon number $\langle P^- P^+ \rangle$ (black dashed curve) by preparing the initial state of the system as $|eee, 0, 0\rangle$. (a) System dynamics with no decay. (b) System dynamics with decay rates $\kappa = \gamma = 2\zeta = 1\times10^{-4}\omega_0$. Other parameters are $\eta g/\omega_0 = 0.06$ and $\nu/\omega_0 = 1.5$.

exponentials will go zero [42]. Only considering the energy levels of the system with all transitions having different frequencies, we then can neglect all fast oscillating terms. In the text, the system consists of three subsystems ($n = 3$). At zerotemperature $T = 0$ with $\langle O_m O_n \rangle = \mathrm{Tr}_B[O_m O_n \rho_B]$, the nonzero two-time correlation functions are given by $\langle \tilde{B}_1(t)\tilde{B}_1^\dagger(t')\rangle = \kappa\delta(t-t')/2$, $\langle \tilde{B}_2(t)\tilde{B}_2^\dagger(t')\rangle = \zeta\delta(t-t')/2$, and $\langle \tilde{B}_3(t)\tilde{B}_3^\dagger(t')\rangle = \gamma\delta(t-t')/2$, where κ, ζ, and γ are the decay rates of the cavity mode, the vibration mode, and the ions, respectively [22]. In the Schrödinger picture, we finally get the master equation (7).

APPENDIX D: SYSTEM DYNAMICS FOR THREE-ION EXCITATION WITH ONE PHOTON AND ONE PHONON

A small energy splitting means a long periodic time, where such a long evolution time is hard to achieve in realistic experiment. And if the effective coupling strength is close to and sometimes even smaller than the system decay rates, the amplitudes of the mean values will decrease rapidly within one period of the population oscillation when including loss effects. Figure 6 displays the time evolution of the cavity mean photon number $\langle X^- X^+ \rangle$, mean excitation number $\langle C_1^- C_1^+ \rangle$ for ion 1 (coincides with that of ion 2 and 3), the two-ion correlation $S^{(2)} = \langle C_1^- C_2^- C_2^+ C_1^+ \rangle$ (coincides with $\langle C_1^- C_3^- C_3^+ C_1^+ \rangle$ and $\langle C_2^- C_3^- C_3^+ C_2^+ \rangle$), the three-ion correlation $S^{(3)} = \langle C_1^- C_2^- C_3^- C_3^+ C_2^+ C_1^+ \rangle$, and the mean phonon number $\langle P^- P^+ \rangle$ by preparing all ions in their excited states. In an ideal case without decay, the mean photon number is at its maximum and the ion jumps to its ground state. Meanwhile, the mean phonon number close to one gets its maximum. The Rabi oscillations show the reversible excitation exchange. We observe that the single-ion excitations $\langle C_i^- C_i^+ \rangle$ and $S^{(2)}$, $S^{(3)}$ approximately coincide at any time. This almost-perfect three-ion correlation is a clear signature of the joint excitation. When taking loss effects into consideration, the mean values, which decrease exponentially as expected, still oscillate in cosine or sine form. As expected, the three-ion correlation is more fragile to losses than two-ion correlation, which are all more fragile to losses than $\langle C_i^- C_i^+ \rangle$ [4].

To simulate more realistic scenes, three excited ions are needed to prepare the initial state as $|eee, 0, 0\rangle$, or one can inject both a single photon and a single phonon to prepare the initial state as $|ggg, 1, 1\rangle$. While for a situation that one photon can simultaneously excite three ions and one phonon, only a single photon is needed to be injected by applying a Gaussian pulse to prepare the initial state as $|ggg, 1, 0\rangle$. In the injection process, the additional nonlinearity such as Kerr, cross-Kerr, and Pockels effects need to be taken into consideration [4–6].

APPENDIX E: MODEL GENERALIZATION

With the rapid development in circuit QED systems, optomechanical systems and optical lattices, our model can be further generalized to various experimental platforms by coupling qubits to two bosonic modes. For example, the ionic vibration mode here can be equivalent to the phonon mode of a mechanical resonator in hybrid optomechanical systems [64]. The interaction between two-level atoms and an optical cavity can be described by Rabi model through the Hamiltonian

$$H_{\mathrm{int}} = g(J_+ + J_-)(b^\dagger + b), \tag{E1}$$

where $g = -\mathbf{d}\cdot\varepsilon_0$ is the atom-photon coupling strength. Consider a standard dispersively coupled optomechanical system with the frequency of a mechanical resonator ν and phonon annihilation operator a, in which the resonator's displacement $x = x_{zpf}(a + a^\dagger)$ (x_{zpf} is the zero-point motion amplitude) creates spatial influence on the cavity field (see details in Ref. [64]). Thus, the atom-photon coupling strength g becomes dependent on the mechanical position. Expanded to the first order in x, $g(x) = g(0) + \gamma(a + a^\dagger)$, where $\gamma = (\partial g/\partial x)|_{x=0} x_{zpf}$. Inserting $g(x)$ into the Hamiltonian (E1) and taking $g(0) = 0$, an atom-photon-phonon coupling arise, which is termed *mode field coupling* (MFC). The interaction Hamiltonian becomes

$$H_{\mathrm{int}} = \gamma(a + a^\dagger)(J_+ + J_-)(b^\dagger + b), \tag{E2}$$

which is the only possible interaction allowing the swap of excitation between three quantum systems. This effective MFC interaction Hamiltonian [Eq. (E2)] from hybrid optomechanical systems can also realize three-photon resonance and three-ion excitation.

[1] M. O. Scully and M. S. Zubairy, *Quantum Optics* (Cambridge University Press, Cambridge, 1997).

[2] M. Göppert-Mayer, Über elementarakte mit zwei quantensprüngen, Ann. Phys. **401**, 273 (1931).

[3] L. Garziano, R. Stassi, V. Macrì, A. F. Kockum, S. Savasta, and F. Nori, Multiphoton quantum Rabi oscillations in ultrastrong cavity QED, Phys. Rev. A **92**, 063830 (2015).

[4] L. Garziano, V. Macrì, R. Stassi, O. D. Stefano, and F. Nori, One Photon Can Simultaneously Excite Two or More Atoms, Phys. Rev. Lett. **117**, 043601 (2016).

[5] X. Wang, A. Miranowicz, H.-R. Li, and F. Nori, Observing pure effects of counter-rotating terms without ultrastrong coupling: A single photon can simultaneously excite two qubits, Phys. Rev. A **96**, 063820 (2017).

[6] A. F. Kockum, A. Miranowicz, V. Macrì, S. Savasta, and F. Nori, Deterministic quantum nonlinear optics with single atoms and virtual photons, Phys. Rev. A **95**, 063849 (2017).

[7] J. I. Cirac and P. Zoller, Quantum Computations with Cold Trapped Ions, Phys. Rev. Lett. **74**, 4091 (1995).

[8] A. Sørensen and K. Mølmer, Quantum Computation with Ions in Thermal Motion, Phys. Rev. Lett. **82**, 1971 (1999).

[9] M. Feng and X. Wang, Implementation of quantum gates and preparation of entangled states in cavity QED with cold trapped ions, J. Opt. B: Quantum Semiclass. Opt. **4**, 283 (2002).

[10] S.-Y. Ye and S.-B. Zheng, Scheme for reliable realization of quantum logic gates for two atoms separately trapped in two distant cavities via optical fibers, Opt. Commun. **281**, 1306 (2008).

[11] M. Waseem, M. Irfan, and S. Qamar, Realization of quantum gates with multiple control qubits or multiple target qubits in a cavity, Quantum Inf Process **14**, 1869 (2015).

[12] C. Monroe, Quantum information processing with atoms and photons, Nature (London) **416**, 238 (2002).

[13] R. Blatt and C. F. Roos, Quantum simulations with trapped ions, Nat. Phys. **8**, 277 (2012).

[14] Q. Guo, S.-B. Zheng, J. Wang, C. Song, P. Zhang, K. Li, W. Liu, H. Deng, K. Huang, D. Zheng, X. Zhu, H. Wang, C.-Y. Lu, and J.-W. Pan, Dephasing-Insensitive Quantum Information Storage and Processing with Superconducting Qubits, Phys. Rev. Lett. **121**, 130501 (2018).

[15] W. Kaiser and C. G. B. Garrett, Two-Photon Excitation in CaF_2:Eu^{2+}, Phys. Rev. Lett. **7**, 229 (1961).

[16] B. R. Mollow, Two-photon absorption and field correlation functions, Phys. Rev. **175**, 1555 (1968).

[17] J. Gea-Banacloche, Two-photon absorption of nonclassical light, Phys. Rev. Lett. **62**, 1603 (1989).

[18] M. Rumi and J. W. Perry, Two-photon absorption: an overview of measurements and principles, Adv. Opt. Photon. **2**, 451 (2010).

[19] M. Pawlicki, H. A. Collins, R. G. Denning, and H. L. Anderson, Two-photon absorption and the design of two-photon dyes, Angew. Chem. Int. Ed. **48**, 3244 (2009).

[20] S. Kawata, H.-B. Sun, T. Tanaka, and K. Takada, Finer features for functional microdevices, Nature (London) **412**, 697 (2001).

[21] P. T. C. So, C. Y. Dong, B. R. Masters, and K. M. Berland, Two-Photon Excitation Fluorescence Microscopy, Annu. Rev. Biomed. Eng. **2**, 399 (2000).

[22] K. K. W. Ma and C. K. Law, Three-photon resonance and adiabatic passage in the large-detuning Rabi model, Phys. Rev. A **92**, 023842 (2015).

[23] C. E. Wieman, D. E. Pritchard, and D. J. Wineland, Atom cooling, trapping, and quantum manipulation, Rev. Mod. Phys. **71**, S253 (1999).

[24] W. Paul, Electromagnetic traps for charged and neutral particles, Rev. Mod. Phys. **62**, 531 (1990).

[25] A. Ashkin, Optical trapping and manipulation of neutral particles using lasers, Proc. Natl. Acad. Sci. USA **94**, 4853 (1997).

[26] D. Leibfried, R. Blatt, C. Monroe, and D. Wineland, Quantum dynamics of single trapped ions, Rev. Mod. Phys. **75**, 281 (2003).

[27] W. Shao, F. Wang, X.-L. Feng, and C. H. Oh, Ionic vibration induced transparency and Autler-Townes splitting, Laser Phys. Lett. **14**, 045203 (2017).

[28] V. Bužek, G. Drobný, M. S. Kim, G. Adam, and P. L. Knight, Cavity QED with cold trapped ions, Phys. Rev. A **56**, 2352 (1997).

[29] R. Rangel, E. Massoni, and N. Zagury, Dynamics of a single trapped ion inside a nonideal QED cavity at zero temperature, Phys. Rev. A **69**, 023805 (2004).

[30] H. Walther, B. T. H. Varcoe, B.-G. Englert, and T. Becker, Cavity quantum electrodynamics, Rep. Prog. Phys. **69**, 1325 (2006).

[31] A. Mortezapour, G. Naeimi, and R. L. Franco, Coherence and entanglement dynamics of vibrating qubits, Opt. Commun. **424**, 26 (2018).

[32] H. Zeng and F. Lin, Quantum conversion between the cavity fields and the center-of-mass motion of ions in a quantized trap, Phys. Rev. A **50**, R3589(R) (1994).

[33] F. L. Semião, A. Vidiella-Barranco, and J. A. Roversi, Entanglement between motional states of a single trapped ion and light, Phys. Rev. A **64**, 024305 (2001).

[34] X.-L. Feng, Y. Xu, and C. H. Oh, Cavity quantum electrodynamics with rapidly vibrating atom, Laser Phys. Lett. **11**, 025204 (2014).

[35] B. E. King, C. S. Wood, C. J. Myatt, Q. A. Turchette, D. Leibfried, W. M. Itano, C. Monroe, and D. J. Wineland, Cooling the Collective Motion of Trapped Ions to Initialize a Quantum Register, Phys. Rev. Lett. **81**, 1525 (1998).

[36] L. D. Landau and E. M. Lifshitz, *Quantum Mechanics: Non-Relativistic Theory* (Butterworth-Heinemann, Oxford, UK, 1981).

[37] P. Forn-Díaz, L. Lamata, E. Rico, J. Kono, and E. Solano, Ultrastrong coupling regimes of light-matter interaction, Rev. Mod. Phys. **91**, 025005 (2019).

[38] A. F. Kockum, A. Miranowicz, S. D. Liberato, S. Savasta, and F. Nori, Ultrastrong coupling between light and matter, Nat. Rev. Phys. **1**, 19 (2019).

[39] N. K. Langford, R. Sagastizabal, M. Kounalakis, C. Dickel, A. Bruno, F. Luthi, D. J. Thoen, A. Endo, and L. DiCarlo, Experimentally simulating the dynamics of quantum light and matter at deep-strong coupling, Nat. Commun. **8**, 1715 (2017).

[40] The general form of the effective Hamiltonian is $H_{\rm eff} = -\frac{\Omega_{\rm eff}}{\sqrt{6}}[a^\dagger a a^\dagger b^3 \sigma_+ + a a^\dagger a (b^\dagger)^3 \sigma_-]$ with $\Omega_{\rm eff}$ being Eq. (4), the effective coupling strength between the bare states $|g, m, n\rangle$ and $|e, m-3, n+1\rangle$ is $(n+1)\sqrt{(n+1)m(m-1)(m-2)/6}\Omega_{\rm eff}$. See arXiv:2206.12221 for more details.

[41] W. Shao, C. Wu, and X.-L. Feng, Generalized James' effective Hamiltonian method, Phys. Rev. A **95**, 032124 (2017).

[42] F. Beaudoin, J. M. Gambetta, and A. Blais, Dissipation and ultrastrong coupling in circuit QED, Phys. Rev. A **84**, 043832 (2011).

[43] A. Settineri, V. Macrì, A. Ridolfo, O. D. Stefano, A. F. Kockum, F. Nori, and S. Savasta, Dissipation and thermal noise in hybrid quantum systems in the ultrastrong-coupling regime, Phys. Rev. A **98**, 053834 (2018).

[44] V. Macrì, A. Ridolfo, O. D. Stefano, A. F. Kockum, F. Nori, and S. Savasta, Nonperturbative Dynamical Casimir Effect in Optomechanical Systems: Vacuum Casimir-Rabi Splittings, Phys. Rev. X **8**, 011031 (2018).

[45] M. Yin, Mechanical oscillator can excite an atom through the quantum vacuum, arXiv:2106.14206.

[46] A. F. Kockum, V. Macrì, L. Garziano, S. Savasta, and F. Nori, Frequency conversion in ultrastrong cavity QED, Sci. Rep. **7**, 5313 (2017).

[47] L. Hornekær, N. Kjærgaard, A. M. Thommesen, and M. Drewsen, Structural Properties of Two-Component Coulomb Crystals in Linear Paul Traps, Phys. Rev. Lett. **86**, 1994 (2001).

[48] C. Cormick and G. Morigi, Ion chains in high-finesse cavities, Phys. Rev. A **87**, 013829 (2013).

[49] Y. Xie, X. Zhang, B. Ou, T. Chen, J. Zhang, C. Wu, W. Wu, and P. Chen, Creating equally spaced linear ion string in a surface-electrode trap by feedback control, Phys. Rev. A **95**, 032341 (2017).

[50] S. R. Jefferts, C. Monroe, E. W. Bell, and D. J. Wineland, Coaxial-resonator-driven rf (Paul) trap for strong confinement, Phys. Rev. A **51**, 3112 (1995).

[51] G. R. Guthöhrlein, M. Keller, K. Hayasaka, W. Lange, and H. Walther, A single ion as a nanoscopic probe of an optical field, Nature (London) **414**, 49 (2001).

[52] D. R. Leibrandt, J. Labaziewicz, V. Vuletić, and I. L. Chuang, Cavity Sideband Cooling of a Single Trapped Ion, Phys. Rev. Lett. **103**, 103001 (2009).

[53] M. Weidinger, B. T. H. Varcoe, R. Heerlein, and H. Walther, Trapping States in the Micromaser, Phys. Rev. Lett. **82**, 3795 (1999).

[54] J.-M. Pirkkalainen, S. U. Cho, F. Massel, J. Tuorila, T. T. Heikkilä, P. J. Hakonen, and M. A. Sillanpää, Cavity optomechanics mediated by a quantum two-level system, Nat. Commun. **6**, 6981 (2015).

[55] C. Zhao, R. Peng, Z. Yang, S. Chao, C. Li, and L. Zhou, Atom-mediated phonon blockade and controlled-z gate in superconducting circuit system, Ann. Phys. **533**, 2100039 (2021).

[56] C. Rigetti, J. M. Gambetta, S. Poletto, B. L. T. Plourde, J. M. Chow, A. D. Córcoles, J. A. Smolin, S. T. Merkel, J. R. Rozen, G. A. Keefe, M. B. Rothwell, M. B. Ketchen, and M. Steffen, Superconducting qubit in a waveguide cavity with a coherence time approaching 0.1 ms, Phys. Rev. B **86**, 100506(R) (2012).

[57] X. Y. Jin, A. Kamal, A. P. Sears, T. Gudmundsen, D. Hover, J. Miloshi, R. Slattery, F. Yan, J. Yoder, T. P. Orlando, S. Gustavsson, and W. D. Oliver, Thermal and Residual Excited-State Population in a 3D Transmon Qubit, Phys. Rev. Lett. **114**, 240501 (2015)

[58] P. F. Herskind, A. Dantan, J. P. Marler, M. Albert, and M. Drewsen, Realization of collective strong coupling with ion Coulomb crystals in an optical cavity, Nat. Phys. **5**, 494 (2009).

[59] J. Pedregosa-Gutierrez and M. Mukherjee, Realisation of homogeneous ion chain using surface traps, arXiv:2106.14678.

[60] C. H. Tseng, S. Somaroo, Y. Sharf, E. Knill, R. Laflamme, T. F. Havel, and D. G. Cory, Quantum simulation of a three-body-interaction Hamiltonian on an NMR quantum computer, Phys. Rev. A **61**, 012302 (1999).

[61] J. K. Pachos and E. Rico, Effective three-body interactions in triangular optical lattices, Phys. Rev. A **70**, 053620 (2004).

[62] P. R. Johnson, E. Tiesinga, J. V. Porto, and C. J. Williams, Effective three-body interactions of neutral bosons in optical lattices, New J. Phys. **11**, 093022 (2009).

[63] M. Aspelmeyer, T. J. Kippenberg, and F. Marquardt, Cavity optomechanics, Rev. Mod. Phys. **86**, 1391 (2014).

[64] M. Cotrufo and A. Fiore, Coherent Atom-Phonon Interaction through Mode Field Coupling in Hybrid Optomechanical Systems, Phys. Rev. Lett. **118**, 133603 (2017).

[65] M. J. A. Schuetz, E. M. Kessler, G. Giedke, L. M. K. Vandersypen, M. D. Lukin, and J. I. Cirac, Universal Quantum Transducers Based on Surface Acoustic Waves, Phys. Rev. X **5**, 031031 (2015).